

B meson decays to vector charmonium(like) states and a K meson: the role of final-state interactions

Qi-Wei Yuan,^{1,2} Qi Wu,^{3,*} and Ming-Zhu Liu^{1,2,†}

¹*Frontiers Science Center for Rare Isotopes, Lanzhou University, Lanzhou 730000, China*

²*School of Nuclear Science and Technology, Lanzhou University, Lanzhou 730000, China*

³*Institute of Particle and Nuclear Physics, Henan Normal University, Xinxiang 453007, China*

A series of vector charmonium(like) states, accompanied by a K meson, have been observed in the decays of B meson. These processes are color-suppressed at the quark level, as inferred from topological diagram analysis. In this work, we calculate the branching fractions of the decays $B \rightarrow \psi K$, where ψ denotes the charmonium(like) states $\psi(1S)$, $\psi(2S)$, $\psi(4040)$, $\psi(3770)$, and $\psi(4160)$. Our analysis incorporates both short-distance (naive factorization approach) and long-distance (final-state interactions) contributions. Within reasonable parameters, our results align with experimental data except for the $\psi(4160)$, suggesting its possible exotic nature. Furthermore, we find that long-distance contributions dominate these decay processes, highlighting the crucial role of final-state interactions in the productions of charmonium(like) states in B decays.

* Corresponding author:wuqi@htu.edu.cn

† Corresponding author:liumz@lzu.edu.cn

I. INTRODUCTION

With the large data samples collected by B factories and LHCb experiments, B meson decays have become an ideal platform for precisely testing the Standard Model and searching for new physics signals [1, 2]. Surprisingly, many new hadron states beyond the conventional mesons and baryons in the quark model, also known as exotic states, have been observed in b -flavored hadron decays, which provide the opportunity to deeply study the non-perturbative hadron interaction as well as explore the existence of hadrons with unconventional configurations [3]. Over the past two decades, revealing the nature of these exotic states has been a primary focus for both experimentalists and theorists. However, their underlying structure remains highly debated [4–17]. Among them, the charmoniumlike states as one of the major categories motivate intensive discussions on their internal structure and properties [14].

The recent studies show that the charmoniumlike states have strong couplings to a pair of charmed mesons. The unquenched quark model has been utilized to analyze the mass spectra of charmoniumlike states, demonstrating that the inclusion of charmed meson pair effects significantly reduces the discrepancies between theoretical predictions and experimental measurements [18–23]. On the other hand, the spectra of these states can also be described at the hadron level with the hadron-hadron interaction dressed by the presence of bare states [24–28]. Moreover, the strong decays of charmoniumlike states have shown that charmed meson pairs play a crucial role in explaining the experimental observations [29–32]. It is evident that hadronic molecule components and bare components are intricately mixed in charmoniumlike states, and these two components may compete in the formation of such states. For some states near the mass thresholds of charmed meson pairs such as $X(3872)$ [33], the hadronic molecule components account for a significant proportion [34, 35], which are even regarded as pure hadronic molecules.

It is natural to investigate the internal structure of the charmoniumlike states through B meson decays. However, calculating their branching fractions at the quark level is challenging due to the intricate non-perturbative effects and the ambiguous internal structures of charmoniumlike states [36]. The production of the $X(3872)$ in B meson decay has been garnered significant interest. In Ref. [37], Meng et al., adopted the QCD factorization approach well explaining the absolute branching fraction of the decay $B \rightarrow X(3872)K$, but failing to explain the ratio of $\mathcal{B}[B^+ \rightarrow X(3872)K^+] / \mathcal{B}[B^0 \rightarrow X(3872)K^0]$, where $X(3872)$ is assumed to be a $\chi_{c1}(2P)$ state. On the other hand, by assuming $X(3872)$ to be a $\bar{D}D^*$ molecule, we utilized the final state interactions (FSIs) approach to successfully describe both the absolute branching fraction and their ratio [38], suggesting that $X(3872)$ contains a significant molecular component, consistent with experimental analyses [39, 40]. Furthermore, our results indicate that the long-distance contributions dominate the decays $B \rightarrow X(3872)K$, similar to those of other charmoniumlike states [41–43]. The FSIs

TABLE I. Branching fractions (in units of 10^{-4}) for the decays of B mesons into vector charmonium(like) states accompanied by a kaon meson [47].

Decay modes	$\rightarrow \psi(1S)$	$\rightarrow \psi(2S)$	$\rightarrow \psi(4040)$	$\rightarrow \psi(3770)$	$\rightarrow \psi(4160)$
Experiments	10.20 ± 0.19	6.24 ± 0.21	16.0 ± 5.0	4.3 ± 1.1	5.1 ± 2.7

approach has already been extensively utilized to address the non-perturbative effects inherent in the decays of heavy-flavored hadrons [44–46]. In this work, we employ the FSIs approach to study the production of vector charmonium(like) states in B decays.

It should be noted that the number of experimental observations of the vector charmonium(like) states is the largest among all charmonium(like) states [47], and this trend also holds true for their observations in B decays. In Table I, we list the observed experimental branching fractions of the B meson decaying into the vector charmonium(like) states and a K meson. The absolute branching fraction of the decay $B \rightarrow \psi(4415)K$ is absent although $\psi(4415)$ is observed in the decay $B \rightarrow D\bar{D}K$ [47]. According to the potential model [21, 48–50], the charmoniumlike states $\psi(4040)$, $\psi(3770)$, and $\psi(4160)$ are assigned as the $\psi(3S)$, $\psi(1D)$, and $\psi(2D)$ states, where the excited bare components account for large proportion. By analyzing the experimental data [51], $\psi(4040)$ and $\psi(3770)$ are assigned as $\psi(3S)$ and $\psi(1D)$ states, while $\psi(4160)$ and $\psi(4230)$ are assigned as the same state $\psi(2D)$ ¹. Up to now, a unified framework to interpret the branching fractions of the B meson decaying into the vector charmonium(like) states and a K meson, as listed in Table I, is still missing, which is the primary objective of the present work.

This work is organized as follows. In Sec. II, we begin by briefly introducing the tree-level Feynman diagrams and triangle Feynman diagrams, which account for the short-distance and long-distance contributions, respectively, in the decays of the B meson into vector charmonium(like) states and a K meson. We also present the effective Lagrangian approach in this section. The numerical results and discussions are provided in Sec. III. Finally, a summary is given in the last section.

II. THEORETICAL FORMALISM

The decays of the B meson into the vector charmonium(like) states and a K meson (denoted by $B \rightarrow \psi K$) proceed via the quark-level transition $b \rightarrow c\bar{s}$ [54]. From the analysis of the topological diagrams, the decays $B \rightarrow \psi K$ belong to C -type diagrams, which are color suppressed [55, 56]. As indicated in Ref. [57], the nonfactorizable effects responsible for the long-distance contributions are sizable

¹ Unlike $\psi(3770)$, the pole positions of $\psi(4040)$ and $\psi(4160)$ exist large uncertainty [52, 53].

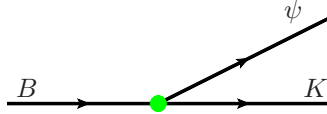


FIG. 1. Tree diagram accounting for short-distance contributions to the decays $B \rightarrow \psi K$ [$\psi(1S)$, $\psi(2S)$, $\psi(4040)$, $\psi(3770)$, and $\psi(4160)$].

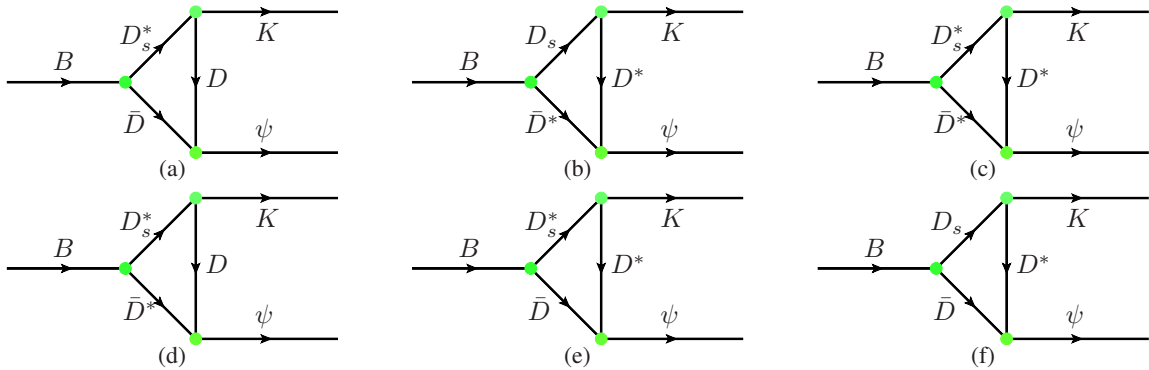


FIG. 2. Triangle diagrams accounting for long-distance contributions to the decays $B \rightarrow \psi K$ [$\psi(1S)$, $\psi(2S)$, $\psi(4040)$, $\psi(3770)$, and $\psi(4160)$]. All diagrams contribute to the productions of $\psi(1S)$, $\psi(2S)$, and $\psi(4040)$ in B decays. Only the diagram (a) contributes to the production of $\psi(3770)$ in B decay, and the diagrams (b-f) contribute to the production of $\psi(4160)$ in B decay.

in these decays. Therefore, following Refs. [46, 58], we consider both the short-distance and long-distance contributions to the decays $B \rightarrow \psi K$. The short-distance contributions are depicted by tree diagrams as shown in Fig. 1, while the long-distance contributions are represented by triangle diagrams [59–61] as shown in Fig. 2.

With the factorization ansatz, the tree diagram of the decays $B \rightarrow \psi K$ can be expressed as the product of two current matrix elements:

$$\mathcal{A}(B \rightarrow \psi K) = \frac{G_F}{\sqrt{2}} V_{cb} V_{cs} a_2 \langle \psi | (c\bar{c})_{V-A} | 0 \rangle \langle K | (s\bar{b})_{V-A} | B \rangle, \quad (1)$$

with $(q\bar{q})_{V-A}$ standing for $q\gamma_\mu(1 - \gamma_5)\bar{q}$. Since the effective Wilson coefficient a_2 depends on the renormalization energy scale, we adopt the value of a_2 at the mass of bottom quark, i.e., $a_2 = 0.102$ [62]. In this work, we take the values of $G_F = 1.166 \times 10^{-5}$ GeV $^{-2}$, $V_{cb} = 0.041$, $V_{cs} = 0.987$. The current matrix element for the ψ meson created from the vacuum is parameterized as [63, 64]

$$\langle \psi | (c\bar{c})_{V-A} | 0 \rangle = f_\psi m_\psi \varepsilon_\mu^*, \quad (2)$$

where f_ψ is the decay constant of a ψ meson. Given the electronic width of a ψ meson, one can derive its

TABLE II. f_ψ decay constants of the vector charmonium(like) states.

States	$\psi(1S)$	$\psi(2S)$	$\psi(4040)$	$\psi(3770)$	$\psi(4160)$
Decay Constants(MeV)	415.49	294.03	186.81	99.67	141.83

decay constant via [42, 65]

$$f_\psi = \sqrt{\frac{3m_\psi \Gamma^{\psi \rightarrow e^+e^-}}{4\pi\alpha^2 e_q^2}}, \quad (3)$$

where α is the fine-structure constant. The decay constants of $\psi(1S)$, $\psi(2S)$, $\psi(4040)$, $\psi(3770)$, and $\psi(4160)$ mesons are presented in Table II. The current matrix element of $\langle K|(s\bar{b})_{V-A}|B\rangle$ describing the hadronic transitions is parameterized by following form factors:

$$\langle K|(s\bar{b})_{V-A}|B\rangle = \left[P^\mu - \frac{m_B^2 - m_K^2}{q^2} q^\mu \right] F_1(q^2) + \frac{m_B^2 - m_K^2}{q^2} q^\mu F_0(q^2), \quad (4)$$

with F_0 and F_1 being the form factors for $B(k_0) \rightarrow K(p_1)$, where $P = k_0 + p_1$ and $q = k_0 - p_1$. The form factors F_0 and F_1 are parameterized as

$$F(q^2) = \frac{F(0)}{1 - a\zeta + b\zeta^2}, \quad (5)$$

with $\zeta = q^2/m_B^2$, where the values of parameters $F(0)$, a , and b are extracted by the covariant light-front quark model [64], listing in Table III.

With the above effective Lagrangian, we obtain the amplitude of the decays $B(k_0) \rightarrow \psi(q)K(p_1)$ in Fig. 1 as

$$\mathcal{A}(B \rightarrow \psi K) = \frac{G_F}{\sqrt{2}} V_{cb} V_{cs} a_2 f_\psi m_\psi (k_0 + p_1) \cdot \varepsilon(p_2) F_1(q^2). \quad (6)$$

For the weak interaction vertices of triangle diagrams in Fig. 2, the decay amplitudes of $B(k_0) \rightarrow D_s^{(*)}(q_1)\bar{D}^{(*)}(q_2)$ can be expressed as the products of two current matrix elements [66, 67]

$$\mathcal{A}(B \rightarrow D_s \bar{D}^*) = \frac{G_F}{\sqrt{2}} V_{cb} V_{cs} a_1 \langle D_s | (s\bar{c})_{V-A} | 0 \rangle \langle \bar{D}^* | (c\bar{b})_{V-A} | B \rangle, \quad (7)$$

$$\mathcal{A}(B \rightarrow D_s \bar{D}) = \frac{G_F}{\sqrt{2}} V_{cb} V_{cs} a_1 \langle D_s | (s\bar{c})_{V-A} | 0 \rangle \langle \bar{D} | (c\bar{b})_{V-A} | B \rangle, \quad (8)$$

$$\mathcal{A}(B \rightarrow D_s^* \bar{D}) = \frac{G_F}{\sqrt{2}} V_{cb} V_{cs} a_1 \langle D_s^* | (s\bar{c})_{V-A} | 0 \rangle \langle \bar{D} | (c\bar{b})_{V-A} | B \rangle, \quad (9)$$

$$\mathcal{A}(B \rightarrow D_s^* \bar{D}^*) = \frac{G_F}{\sqrt{2}} V_{cb} V_{cs} a_1 \langle D_s^* | (s\bar{c})_{V-A} | 0 \rangle \langle \bar{D}^* | (c\bar{b})_{V-A} | B \rangle. \quad (10)$$

Similarly, we adopt the effective Wilson coefficient $a_1 = 1.03$ [62]. The former current matrix elements are written as

$$\langle D_s(p_1) | (s\bar{c})_{V-A} | 0 \rangle = i f_{D_s} p_{1\mu}, \quad (11)$$

$$\langle D_s^*(p_1, \epsilon) | (s\bar{c})_{V-A} | 0 \rangle = f_{D_s^*} m_{D_s^*} \epsilon_\mu^*, \quad (12)$$

TABLE III. Values of $F(0)$, a , and b in the $B \rightarrow D^{(*)}$ and $B \rightarrow K$ transition form factors [64].

	V	A_0	A_1	A_2	F_0	F_1		F_0	F_1
$F(0)^{B \rightarrow D^{(*)}}$	0.77	0.68	0.65	0.61	0.67	0.67	$F(0)^{B \rightarrow K}$	0.34	0.34
$a^{B \rightarrow D^{(*)}}$	1.25	1.21	0.60	1.12	0.63	1.22	$a^{B \rightarrow K}$	0.78	1.60
$b^{B \rightarrow D^{(*)}}$	0.38	0.36	0.00	0.31	-0.01	0.36	$b^{B \rightarrow K}$	0.05	0.73

where the decay constants of D_s and D_s^* are adopted as $f_{D_s} = 250$ MeV and $f_{D_s^*} = 272$ MeV [64, 68–71]. The matrix elements of hadron transitions $B(k_0) \rightarrow \bar{D}^{(*)}(q_2)$ are parameterized by following form factors [63, 64]

$$\langle \bar{D}^* | (c\bar{b})_{V-A} | B \rangle = i\epsilon_\alpha^* \left\{ -g^{\mu\alpha} (m_{\bar{D}^*} + m_B) A_1(q^2) + P^\mu P^\alpha \frac{A_2(q^2)}{m_{\bar{D}^*} + m_B} \right. \quad (13)$$

$$\left. + i\varepsilon^{\mu\alpha\beta\gamma} P_\beta q_\gamma \frac{V(q^2)}{m_{\bar{D}^*} + m_B} + q^\mu P^\alpha \left[\frac{m_{\bar{D}^*} + m_B}{q^2} A_1(q^2) - \frac{m_B - m_{\bar{D}^*}}{q^2} A_2(q^2) - \frac{2m_{\bar{D}^*}}{q^2} A_0(q^2) \right] \right\},$$

$$\langle \bar{D} | (c\bar{b})_{V-A} | B \rangle = \left[P^\mu - \frac{m_B^2 - m_{\bar{D}}^2}{q^2} q^\mu \right] F_1(q^2) + \frac{m_B^2 - m_{\bar{D}}^2}{q^2} q^\mu F_0(q^2), \quad (14)$$

where $q = k_0 - q_2$ and $P = k_0 + q_2$.

With above Lagrangians, the weak decay amplitudes of $B(k_0) \rightarrow D_s^{(*)}(q_1) \bar{D}^{(*)}(q_2)$ have the following form

$$\begin{aligned} \mathcal{A}(B \rightarrow D_s \bar{D}^*) &= -\frac{G_F}{\sqrt{2}} V_{cb} V_{cs} a_1 f_{D_s} \{ -q_1 \cdot \varepsilon(q_2) (m_{\bar{D}^*} + m_B) A_1(q_1^2) \\ &\quad + (k_0 + q_2) \cdot \varepsilon(q_2) q_1 \cdot (k_0 + q_2) \frac{A_2(q_1^2)}{m_{\bar{D}^*} + m_B} + (k_0 + q_2) \cdot \varepsilon(q_2) \\ &\quad [(m_{\bar{D}^*} + m_B) A_1(q_1^2) - (m_B - m_{\bar{D}^*}) A_2(q_1^2) - 2m_{\bar{D}^*} A_0(q_1^2)] \}, \end{aligned} \quad (15)$$

$$\mathcal{A}(B \rightarrow D_s \bar{D}) = i \frac{G_F}{\sqrt{2}} V_{cb} V_{cs} a_1 f_{D_s} (m_B^2 - m_D^2) F_0(q_1^2), \quad (16)$$

$$\mathcal{A}(B \rightarrow D_s^* \bar{D}) = \frac{G_F}{\sqrt{2}} V_{cb} V_{cs} a_1 m_{D_s^*} f_{D_s^*} (k_0 + q_2) \cdot \varepsilon(q_1) F_1(q_1^2), \quad (17)$$

$$\begin{aligned} \mathcal{A}(B \rightarrow D_s^* \bar{D}^*) &= i \frac{G_F}{\sqrt{2}} V_{cb} V_{cs} a_1 m_{D_s^*} f_{D_s^*} \varepsilon_\mu(q_1) \left[(-g^{\mu\alpha} (m_{\bar{D}^*} + m_B) A_1(q_1^2) \right. \\ &\quad \left. + (k_0 + q_2)^\mu (k_0 + q_2)^\alpha \frac{A_2(q_1^2)}{m_{\bar{D}^*} + m_B} + i\varepsilon^{\mu\alpha\beta\gamma} (k_0 + q_2)_\beta q_{1\gamma} \frac{V(q_1^2)}{m_{\bar{D}^*} + m_B} \right] \varepsilon_\alpha(q_2). \end{aligned} \quad (18)$$

The Lagrangians describing the interactions between charmed mesons and the kaon [72]

$$\mathcal{L}_{D_s^* DK} = -ig_{D_s^* DK} (D^\mu K \bar{D}_{s\mu}^* - D_{s\mu}^* \partial^\mu K \bar{D}), \quad (19)$$

$$\mathcal{L}_{D_s D^* K} = -ig_{D_s D^* K} (D_s \partial^\mu K \bar{D}_\mu^* - D_\mu^* \partial^\mu K \bar{D}_s), \quad (20)$$

$$\mathcal{L}_{D_s^* D^* K} = -g_{D_s^* D^* K} \varepsilon_{\mu\nu\alpha\beta} \partial^\mu D_s^{*\nu} \partial^\alpha \bar{D}^{*\beta} K, \quad (21)$$

TABLE IV. Partial widths of the charmoniumlike states decaying into a pair of charmed mesons.

	$\psi(4040)_I$ [47]	$\psi(4040)_{II}$ [52]	$\psi(4160)_I$ [47]	$\psi(4160)_{II}$ [53]	$\psi(3770)$ [47]
Total	84.5 ± 12.3	130 ± 30	69 ± 10	104.83 ± 23.71	27.5 ± 0.9
$\bar{D}D$	14.28 ± 2.08	40.81 ± 9.42	—	27.18 ± 6.15	25.58 ± 0.84
\bar{D}^*D	29.75 ± 4.33	37.79 ± 8.72	8.75 ± 1.26	14.56 ± 3.29	—
\bar{D}^*D^*	10.71 ± 1.56	13.60 ± 3.14	51.49 ± 7.46	48.53 ± 10.98	—

where the couplings are determined as $g_{D_s^*DK} = g_{D_s D^*K} = 14.00 \pm 1.73$ and $g_{D_s^*D^*K} = 8.63 \pm 0.99 \text{ GeV}^{-1}$ via SU(3)-flavor symmetry [73].

The effective Lagrangians accounting for the interactions between the charmonium states and a pair of charmed mesons read [59, 61, 72, 74, 75]

$$\mathcal{L}_{\psi DD} = ig_{\psi DD}\psi_\mu(\partial^\mu D\bar{D} - D\partial^\mu\bar{D}), \quad (22)$$

$$\mathcal{L}_{\psi DD^*} = -g_{\psi DD^*}\epsilon^{\alpha\beta\mu\nu}\partial_\alpha\psi_\beta(\partial_\mu D_\nu^*\bar{D} + D\partial_\mu\bar{D}_\nu^*), \quad (23)$$

$$\begin{aligned} \mathcal{L}_{\psi D^*D^*} = & -ig_{\psi D^*D^*}[\psi^\mu(\partial_\mu D_\nu^*\bar{D}^{*\nu} - D^{*\nu}\partial_\mu\bar{D}_\nu^*) + (\partial_\mu\psi_\nu D^{*\nu} - \psi^\nu\partial_\mu D_\nu^*)\bar{D}^{*\mu} \\ & + D^{*\mu}(\psi^\nu\partial_\mu\bar{D}_\nu^* - \partial_\mu\psi_\nu\bar{D}^{*\nu})], \end{aligned} \quad (24)$$

where the g with subscript are the couplings of the charmonium(like) states to the charmed mesons. There are five vector charmonium(like) states in Table I, which can be categorized into two scenarios. In Scenario I, the $\psi(1S)$ and $\psi(2S)$ as the conventional charmonium states are below the $\bar{D}D$ mass threshold, while Scenario II includes the $\psi(3770)$, $\psi(4040)$, and $\psi(4160)$ as the charmoniumlike states, all of which are above the $\bar{D}D$ mass threshold. For Scenario I, the $\psi(1S)$ and $\psi(2S)$ states are coupled to the $\bar{D}^{(*)}D^{(*)}$ channels. The couplings between J/ψ and $\bar{D}^{(*)}D^{(*)}$ are taken from the QCD sum rules [73], as listed in Table V, while those between $\psi(2S)$ and $\bar{D}^{(*)}D^{(*)}$ are not as straightforward to estimate directly. According to Refs. [76–78], the couplings between J/ψ and $\bar{D}^{(*)}D^{(*)}$ are equal to those of $\psi(2S)$ and $\bar{D}^{(*)}D^{(*)}$. As a result, using the relationship, we obtain the couplings between $\psi(2S)$ and $\bar{D}^{(*)}D^{(*)}$.

For Scenario II, the coupling constants are determined by reproducing the partial decay widths of the charmoniumlike states decaying into a pair of charmed mesons. With the partial width of the decay $\psi(3770) \rightarrow \bar{D}D$ [47], the coupling is determined as $g_{\psi(3770)\bar{D}D} = 18.55^{+0.30}_{-0.31}$, consistent with Refs. [79, 80]. Assuming that the total widths of the $\psi(4040)$ and $\psi(4160)$ states are fully saturated by decaying into a pair of the open charmed mesons [47], their partial decay widths are estimated to be in Table IV. Then, we determine the corresponding couplings (denoted by subscript I) as shown in Table V. It should be noted that the partial decay widths of $\psi(4040)$ and $\psi(4160)$ vary a lot. Therefore, we adopt the

TABLE V. Charmonium(like) states couplings to a pair of charmed mesons.

Couplings	$g_{\psi(1S)\bar{D}D}$	$g_{\psi(1S)\bar{D}^*D}$	$g_{\psi(1S)\bar{D}^*D^*}$	$g_{\psi(2S)\bar{D}D}$	$g_{\psi(2S)\bar{D}^*D}$	$g_{\psi(2S)\bar{D}^*D^*}$
	5.8 ± 0.9	$4.0 \pm 0.6 \text{ GeV}^{-1}$	6.2 ± 0.9	$5.8^{+1.57}_{-1.39}$	$4.0^{+1.06}_{-0.94} \text{ GeV}^{-1}$	$6.2^{+1.64}_{-1.43}$
Couplings	$g_{I\psi(4040)\bar{D}D}$	$g_{I\psi(4040)\bar{D}^*D}$	$g_{I\psi(4040)\bar{D}^*D^*}$	$g_{\psi(3770)\bar{D}D}$	$g_{I\psi(4160)\bar{D}^*D}$	$g_{I\psi(4160)\bar{D}^*D^*}$
	$3.1^{+0.22}_{-0.23}$	$2.47^{+0.17}_{-0.19} \text{ GeV}^{-1}$	$3.56^{+0.25}_{-0.27}$	$18.55^{+0.30}_{-0.31}$	0.81 ± 0.06	1.65 ± 0.12
Couplings	$g_{II\psi(4040)\bar{D}D}$	$g_{II\psi(4040)\bar{D}^*D}$	$g_{II\psi(4040)\bar{D}^*D^*}$	$g_{II\psi(4160)\bar{D}D}$	$g_{II\psi(4160)\bar{D}^*D}$	$g_{II\psi(4160)\bar{D}^*D^*}$
	$5.19^{+0.57}_{-0.64}$	$2.73^{+0.30}_{-0.34} \text{ GeV}^{-1}$	$3.50^{+0.38}_{-0.43}$	$3.47^{+0.37}_{-0.42}$	$1.18^{+0.13}_{-0.14}$	$2.02^{+0.22}_{-0.24}$

partial decay widths of $\psi(4040)$ and $\psi(4160)$ in Ref. [52, 53, 81] to determine the couplings (denoted by subscript II) as shown in Table V.

Using above Lagrangians, the amplitudes of the triangle diagrams in Fig. 2 are written as

$$\begin{aligned} \mathcal{M}_a &= i^2 \int \frac{d^4 q_3}{(2\pi)^4} \left[\mathcal{A}_\mu(B \rightarrow D_s^* \bar{D}) \right] \left[g_{D_s^* DK} p_{1\nu} \right] \left[g_{\psi \bar{D}D}(q_3^\tau - q_2^\tau) \varepsilon_\tau(p_2) \right] \\ &\quad \frac{-g^{\mu\nu} + q_1^\mu q_1^\nu / q_1^2}{q_1^2 - m_1^2} \frac{1}{q_2^2 - m_2^2} \frac{1}{q_3^2 - m_3^2} \mathcal{F}(q_3^2, m_3^2), \end{aligned} \quad (25)$$

$$\begin{aligned} \mathcal{M}_b &= i^2 \int \frac{d^4 q_3}{(2\pi)^4} \left[\mathcal{A}_\mu(B \rightarrow D_s \bar{D}^*) \right] \left[-g_{D_s D^* K} p_{1\alpha} \right] \\ &\quad \left[-g_{\psi \bar{D}^* D^*}(p_2) (g^{\nu\beta}(q_3 - q_2)_\tau - g^{\beta\tau}(p_2 + q_3)_\nu + g^{\tau\nu}(q_2 + p_2)_\beta) \right] \\ &\quad \frac{1}{q_1^2 - m_1^2} \frac{-g^{\mu\nu} + q_2^\mu q_2^\nu / q_2^2}{q_2^2 - m_2^2} \frac{-g^{\alpha\beta} + q_3^\alpha q_3^\beta / q_3^2}{q_3^2 - m_3^2} \mathcal{F}(q_3^2, m_3^2), \end{aligned} \quad (26)$$

$$\begin{aligned} \mathcal{M}_c &= i^2 \int \frac{d^4 q_3}{(2\pi)^4} \left[\mathcal{A}_{\omega\mu}(B \rightarrow D_s^* \bar{D}^*) \right] \left[-g_{D_s^* D^* K} \varepsilon_{\rho\phi\eta\alpha} q_1^\rho q_3^\eta \right] \\ &\quad \left[-g_{\psi \bar{D}^* D^*}(p_2) (g^{\nu\beta}(q_3 - q_2)_\tau - g^{\beta\tau}(p_2 + q_3)_\nu + g^{\tau\nu}(q_2 + p_2)_\beta) \right] \\ &\quad \frac{-g^{\omega\phi} + q_1^\omega q_1^\phi / q_1^2}{q_1^2 - m_1^2} \frac{-g^{\mu\nu} + q_2^\mu q_2^\nu / q_2^2}{q_2^2 - m_2^2} \frac{-g^{\alpha\beta} + q_3^\alpha q_3^\beta / q_3^2}{q_3^2 - m_3^2} \mathcal{F}(q_3^2, m_3^2), \end{aligned} \quad (27)$$

$$\begin{aligned} \mathcal{M}_d &= i^2 \int \frac{d^4 q_3}{(2\pi)^4} \left[\mathcal{A}_{\omega\mu}(B \rightarrow D_s \bar{D}^*) \right] \left[g_{D_s^* DK} p_{1\phi} \right] \left[-g_{\psi \bar{D}^* D}(p_2) \varepsilon_{\alpha\tau\beta\nu} p_2^\alpha q_2^\beta \right] \\ &\quad \frac{-g^{\omega\phi} + q_1^\omega q_1^\phi / q_1^2}{q_1^2 - m_1^2} \frac{-g^{\mu\nu} + q_2^\mu q_2^\nu / q_2^2}{q_2^2 - m_2^2} \frac{1}{q_3^2 - m_3^2} \mathcal{F}(q_3^2, m_3^2), \end{aligned} \quad (28)$$

$$\begin{aligned} \mathcal{M}_e &= i^2 \int \frac{d^4 q_3}{(2\pi)^4} \left[\mathcal{A}_\omega(B \rightarrow D_s^* \bar{D}) \right] \left[-g_{D_s^* D^* K} \varepsilon_{\sigma\phi\lambda\mu} q_1^\sigma q_3^\lambda \right] \left[-g_{\psi \bar{D}^* D}(p_2) \varepsilon_{\alpha\tau\beta\nu} p_2^\alpha q_2^\beta \right] \\ &\quad \frac{-g^{\omega\phi} + q_1^\omega q_1^\phi / q_1^2}{q_1^2 - m_1^2} \frac{1}{q_2^2 - m_2^2} \frac{-g^{\mu\nu} + q_3^\mu q_3^\nu / q_3^2}{q_3^2 - m_3^2} \mathcal{F}(q_3^2, m_3^2), \end{aligned} \quad (29)$$

$$\begin{aligned} \mathcal{M}_f &= i^2 \int \frac{d^4 q_3}{(2\pi)^4} \left[\mathcal{A}(B \rightarrow D_s \bar{D}) \right] \left[-g_{D_s D^* K} p_{1\mu} \right] \left[-g_{\psi \bar{D}^* D}(p_2) \varepsilon_{\alpha\tau\beta\nu} p_2^\alpha q_2^\beta \right] \\ &\quad \frac{1}{q_1^2 - m_1^2} \frac{1}{q_2^2 - m_2^2} \frac{-g^{\mu\nu} + q_3^\mu q_3^\nu / q_3^2}{q_3^2 - m_3^2} \mathcal{F}(q_3^2, m_3^2), \end{aligned} \quad (30)$$

TABLE VI. Masses and quantum numbers of relevant hadrons needed in this work [47].

Hadron	$I(J^P)$	M (MeV)	Hadron	$I(J^P)$	M (MeV)
K^0	$\frac{1}{2}(0^-)$	497.611	K^\pm	$\frac{1}{2}(0^-)$	493.677
\bar{D}^0	$1/2(0^-)$	1864.84	D^-	$1/2(0^-)$	1869.66
\bar{D}^{*0}	$1/2(1^-)$	2006.85	D^{*-}	$1/2(1^-)$	2010.26
D_s^\pm	$0(0^-)$	1968.35	$D_s^{*\pm}$	$0(1^-)$	2112.20
B^\pm	$\frac{1}{2}(0^-)$	5279.41	B^0	$\frac{1}{2}(0^-)$	5279.72
$\psi(1S)$	$0(1^-)$	3096.9 ± 0.006	$\psi(2S)$	$0(1^-)$	3686.097 ± 0.011
$\psi(4040)$	$0(1^-)$	4039.6 ± 4.3	$\psi(3770)$	$0(1^-)$	3773.7 ± 0.7
$\psi(4160)$	$0(1^-)$	4191 ± 5			

where we have introduced a dipole form factor $\mathcal{F}(q^2, \Lambda^2) = \frac{m^2 - \Lambda^2}{q^2 - \Lambda^2}$ to eliminate the ultraviolet divergence of the loop functions and take into account the off-shell effect of exchanged mesons. The parameter Λ can be further parameterized as $\Lambda = m + \alpha \Lambda_{\text{QCD}}$ with $\Lambda_{\text{QCD}} = 0.22$ GeV [58], and m is the mass of the exchanged meson.

With the amplitudes for the weak decays $B \rightarrow \psi K$ given above, one can compute their partial decay widths

$$\Gamma = \frac{1}{2J+1} \frac{1}{8\pi} \frac{|\vec{p}|}{m_B^2} |\overline{M}|^2, \quad (31)$$

where $J = 0$ is the total angular momentum of the initial B meson, the overline indicates the sum over the polarization vectors of final states, and $|\vec{p}|$ is the momentum of either final state in the rest frame of the B meson.

III. RESULTS AND DISCUSSIONS

In Table VI, we tabulate the masses and quantum numbers of relevant particles involved in this work. The only parameter in the present work is the cutoff in the form factor $\mathcal{F}(q^2, \Lambda^2)$, which we parameterize through the dimensionless parameter α . Since this parameter cannot be determined from first principles, we vary it from 1 to 5 to estimate the uncertainties in our calculations, following studies of hadron-hadron interactions [44, 82–84]. Moreover, the uncertainties of the couplings (In Eqs. (19-21) and Table V) in the vertices of the triangle diagrams lead to uncertainties for the final results, and those of weak interactions

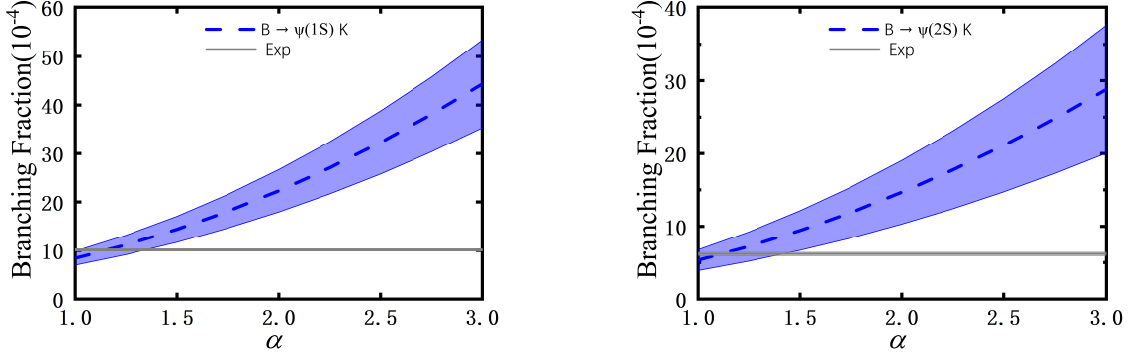


FIG. 3. Branching fractions of the decays $B \rightarrow K\psi(1S)$ and $B \rightarrow K\psi(2S)$ as the function of α . The blue dash line and band correspond to the theoretical central values and uncertainties. The grey straight line and band correspond to the experimental central values and uncertainties.

lead to around 10% uncertainty². As a result, we obtain the uncertainties for the partial decay widths originating from the uncertainties of these couplings via a Monte Carlo sampling within their 1σ intervals. In the following, we present the branching fractions of the decays $B \rightarrow \psi K$.

For the states of Scenario I, we present the branching fractions of the decays of $B \rightarrow \psi(1S)K$ and $B \rightarrow \psi(2S)K$ as a function of α in Fig. 3, where both short-distance and long-distance contributions are taken into account. We can see that the central values of their experimental branching fractions are reproduced when the parameter α is around 1.2, which lies within the reasonable region. Therefore, our model can explain the productions of $\psi(1S)$ and $\psi(2S)$ in B decays. For a comprehensive analysis of each mechanism's contribution to the branching fractions, we individually present the short-distance, long-distance, and total contributions to the decays $B \rightarrow \psi K$ in Table VII. With only the short-distance contributions, the branching fractions of the decays of $B \rightarrow \psi(1S)K$ and $B \rightarrow \psi(2S)K$ are 1.551×10^{-4} and 0.64×10^{-4} , respectively, smaller than the experimental data by one order of magnitude, which implies that the non-factorization effects of these decays are significant. With only long-distance contributions, the branching fractions of the decays of $B \rightarrow \psi(1S)K$ and $B \rightarrow \psi(2S)K$ become larger than those with only short-distance contributions. Once taking into account both short-distance and long-distance contributions, i.e., total contributions, the branching fractions of the decays of $B \rightarrow \psi(1S)K$ and $B \rightarrow \psi(2S)K$ are enhanced since the amplitudes of tree diagrams and triangle diagrams add constructively. From the above analysis, it is demonstrated that the FSIs play a crucial role in the decays of $B \rightarrow \psi(1S)K$ and $B \rightarrow \psi(2S)K$.

For the states of Scenario II, we present the branching fractions of $B \rightarrow \psi(3770)K$, $B \rightarrow \psi(4040)K$,

² The uncertainties of the weak vertices in the triangle diagrams are mainly induced by the $B \rightarrow \bar{D}^{(*)}$ transitions. Using the experimental branching fractions of $\mathcal{B}(B \rightarrow \bar{D}\tau\nu_\tau) = (7.7 \pm 2.5) \times 10^{-3}$ and $\mathcal{B}(B \rightarrow \bar{D}^*\tau\nu_\tau) = (1.88 \pm 0.20)\%$, we find that the form factors of $B \rightarrow \bar{D}^{(*)}$ in Table III have 10% uncertainties.

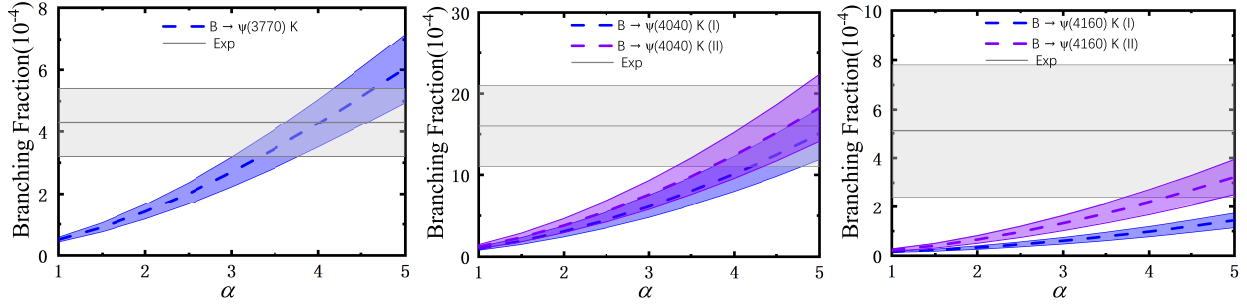


FIG. 4. Branching fractions of $B \rightarrow K\psi(3770)$, $B \rightarrow K\psi(4040)$, and $B \rightarrow K\psi(4160)$ as the function of α . The blue line and horizontal band denote the relevant experimental measurement. The purple line represents the results obtained by using the masses and decay widths retrieved from Refs. [52, 53, 81] as input for the calculations.

and $B \rightarrow \psi(4160)K$ decays as a function of α in Fig. 4. Different from those of Scenario I, larger values of the parameter α are necessary to explain the experimental data. Using the couplings $g_{\psi\bar{D}^{(*)}D^{(*)}}$ from Ref. [47], we find the parameter α to be around 4, 5, and 11.5 for the decays of $B \rightarrow \psi(3770)K$, $B \rightarrow \psi(4040)K$, and $B \rightarrow \psi(4160)K$, respectively. These values correspond to the blue line and band in Fig. 4. In contrast to the $\psi(3770)$ state, the widths of the $\psi(4040)$ and $\psi(4160)$ states are still under debate. Using the results from Refs. [52, 53] as inputs, we recalculate the branching fractions for $B \rightarrow \psi(4040)K$ and $B \rightarrow \psi(4160)K$ decays, shown as the purple line and band in Fig. 4. Notably, the parameter α decreases to approximately 4.5 and 6.5 for the $B \rightarrow \psi(4040)K$ and $B \rightarrow \psi(4160)K$ decays. Therefore, the productions of $\psi(3770)$ and $\psi(4040)$ in B decays can be explained in our model. However, the parameter α for the decay $B \rightarrow \psi(4160)K$ remains unnatural in our model³, which also supports the exotic nature of $\psi(4160)$ from the perspective of B decays, similar to the conclusions obtained from analyzing the invariant mass distributions [51].

Similar to the states of Scenario I, we separately list the short-distance, long-distance, and total contributions to the decays of $B \rightarrow \psi(3770)K$, $B \rightarrow \psi(4040)K$, and $B \rightarrow \psi(4160)K$ in Table VII. The short-distance contributions alone yield branching fractions of $\mathcal{B}[B \rightarrow \psi(3770)K] = 7.0 \times 10^{-6}$, $\mathcal{B}[B \rightarrow \psi(4160)K] = 9.0 \times 10^{-6}$, and $\mathcal{B}[B \rightarrow \psi(4040)K] = 1.93 \times 10^{-5}$, which are nearly two orders of magnitude smaller than the experimental values. This significant discrepancy indicates the importance of non-factorizable effects in these decay processes. In contrast, the long-distance contributions dominant the decay amplitudes, producing substantially larger branching fractions. When incorporating both short-distance and long-distance contributions coherently, we find the enhancement in the branching fractions due to constructive interference between the two amplitudes. However, the interferent effect is not as prominent,

³ Assuming $\psi(4160)$ and $Y(4230)$ as same states, $\psi(4160)$ would have strong coupling to $\bar{D}D_1$, implying that weak vertices $B \rightarrow \bar{D}^{(*)}D_1$ combining the FSIs [42] would contribute to the branching fractions of the decay $B \rightarrow \psi(4160)K$ and change the parameter α in the reasonable region.

TABLE VII. Branching fractions (10^{-4}) of B meson decaying into vector charmonium(like) states and kaon meson.

Decay modes	Short-distance	Long-distance	Total	Experiments
$\rightarrow \psi(1S)$	1.551	$2.818 \sim 89.519$	$8.402 \sim 112.177$	10.20 ± 0.19
$\rightarrow \psi(2S)$	0.640	$2.299 \sim 59.555$	$5.351 \sim 71.948$	6.24 ± 0.21
$\rightarrow \psi(4040)$	0.193	$0.331 \sim 11.847$	$1.006 \sim 15.019$	16.0 ± 5.0
		$0.432 \sim 14.809$	$1.185 \sim 18.267$	
$\rightarrow \psi(3770)$	0.070	$0.269 \sim 5.954$	$0.508 \sim 6.048$	4.3 ± 1.1
$\rightarrow \psi(4160)$	0.090	$0.010 \sim 0.809$	$0.161 \sim 1.437$	5.1 ± 2.7
		$0.035 \sim 2.216$	$0.247 \sim 3.228$	

indicating that FSIs play a dominant role in the processes of the $B \rightarrow \psi(3770)K$, $B \rightarrow \psi(4040)K$, and $B \rightarrow \psi(4160)K$ decays.

As indicated in [85], the ratio of C -type topology diagram to T -type topology diagram is estimated to be $\frac{|C|}{|T|} \sim \mathcal{O}\frac{\Lambda_{QCD}^{hadron}}{m_Q}$. This ratio is approximately unity in charm decays but reduces to $1/4$ in bottom decays, demonstrating less pronounced color suppressed effects in bottom hadron decays compared to charm hadron decays, which is identified by the experimental branching fraction measurements. Nevertheless, the non-factorization effects in bottomed hadron decays are still sizable [46, 86, 87]. Our results in Table VII reveal that the non-factorization effects are significant in the decays of the B meson into the vector charmonium(like) states and a K meson. This provides compelling evidence for the dominant role of FSIs in these processes. In particular, the non-factorization effects in the $B \rightarrow \psi(3770)K$, $B \rightarrow \psi(4040)K$, and $B \rightarrow \psi(4160)K$ decays are more prominent than those in $B \rightarrow \psi(1S)K$ and $B \rightarrow \psi(2S)K$ decays.

IV. SUMMARY AND DISCUSSION

The decays of the B meson into a series of vector charmonium(like) states and a K meson have been observed, providing new opportunities to investigate the nature of charmonium(like) states and their production mechanisms in B decays. In this work, we focused on the decays $B \rightarrow \psi K$ (where ψ denotes $\psi(1S)$, $\psi(2S)$, $\psi(4040)$, $\psi(3770)$, and $\psi(4160)$), for which the branching fractions have been experimentally measured. We analyzed both short-distance and long-distance contributions to these decays, illustrated by the tree diagrams and triangle diagrams, respectively. The short-distance contributions are evaluated within the framework of naive factorization, whereas the long-distance contributions are investigated through FSIs. Using the effective Lagrangian approach, we systematically calculated both the short-distance and long-

distance contributions to the $B \rightarrow \psi K$ decays.

In our model, the experimental branching fractions of $B \rightarrow \psi(1S)K$ and $B \rightarrow \psi(2S)K$ decays are reproduced with $\alpha \approx 1$, while those of $B \rightarrow \psi(3770)K$ and $B \rightarrow \psi(4040)K$ decays require $\alpha \approx 4$. However, the branching fraction of the decay $B \rightarrow \psi(4160)K$ can only be accommodated with an unnaturally large α , implying the exotic nature of $\psi(4160)$ from the perspective of B decays. The dominant uncertainty in our model arises from the couplings between the charmonium(like) states and $\bar{D}^{(*)}D^{(*)}$, which lead to the uncertainties of our results. However, the decay constants of these vector charmonium(like) states are determined directly from their electronic decay widths, ensuring that the results calculated by only short-distance contributions remain robust. Since results within only short-distance contributions play minor role in these decays, we infer that the role of long-distance contributions to these decays are more prominent. Therefore, we conclude that the FSIs play the dominant role in $B \rightarrow \psi K$ decays. Our findings justify studying the production of charmoniumlike states in B decays via FSIs, reinforcing the importance of this mechanism in understanding such charmoniumlike states.

V. ACKNOWLEDGMENTS

We are grateful to Li-Sheng Geng, Qin Chang, Fu-Sheng Yu, Li-Ting Wang, and Zhu-Ding Duan for useful discussions. This work is supported by the National Natural Science Foundation of China under Grants Nos.12105007 and 12405093, as well as supported, in part, by National Key Research and Development Program under Grant No.2024YFA1610504.

- [1] A. A. Alves, Jr. *et al.* (LHCb), JINST **3**, S08005 (2008).
- [2] W. Altmannshofer *et al.* (Belle-II), PTEP **2019**, 123C01 (2019), [Erratum: PTEP 2020, 029201 (2020)], arXiv:1808.10567 [hep-ex].
- [3] N. Brambilla *et al.*, Eur. Phys. J. C **71**, 1534 (2011), arXiv:1010.5827 [hep-ph].
- [4] H.-X. Chen, W. Chen, X. Liu, and S.-L. Zhu, Phys. Rept. **639**, 1 (2016), arXiv:1601.02092 [hep-ph].
- [5] R. F. Lebed, R. E. Mitchell, and E. S. Swanson, Prog. Part. Nucl. Phys. **93**, 143 (2017), arXiv:1610.04528 [hep-ph].
- [6] E. Oset *et al.*, Int. J. Mod. Phys. E **25**, 1630001 (2016), arXiv:1601.03972 [hep-ph].
- [7] A. Esposito, A. Pilloni, and A. D. Polosa, Phys. Rept. **668**, 1 (2017), arXiv:1611.07920 [hep-ph].
- [8] Y. Dong, A. Faessler, and V. E. Lyubovitskij, Prog. Part. Nucl. Phys. **94**, 282 (2017).
- [9] F.-K. Guo, C. Hanhart, U.-G. Meißner, Q. Wang, Q. Zhao, and B.-S. Zou, Rev. Mod. Phys. **90**, 015004 (2018), [Erratum: Rev.Mod.Phys. 94, 029901 (2022)], arXiv:1705.00141 [hep-ph].

- [10] S. L. Olsen, T. Skwarnicki, and D. Zieminska, Rev. Mod. Phys. **90**, 015003 (2018), arXiv:1708.04012 [hep-ph].
- [11] A. Ali, J. S. Lange, and S. Stone, Prog. Part. Nucl. Phys. **97**, 123 (2017), arXiv:1706.00610 [hep-ph].
- [12] M. Karliner, J. L. Rosner, and T. Skwarnicki, Ann. Rev. Nucl. Part. Sci. **68**, 17 (2018), arXiv:1711.10626 [hep-ph].
- [13] F.-K. Guo, X.-H. Liu, and S. Sakai, Prog. Part. Nucl. Phys. **112**, 103757 (2020), arXiv:1912.07030 [hep-ph].
- [14] N. Brambilla, S. Eidelman, C. Hanhart, A. Nefediev, C.-P. Shen, C. E. Thomas, A. Vairo, and C.-Z. Yuan, Phys. Rept. **873**, 1 (2020), arXiv:1907.07583 [hep-ex].
- [15] L. Meng, B. Wang, G.-J. Wang, and S.-L. Zhu, Phys. Rept. **1019**, 1 (2023), arXiv:2204.08716 [hep-ph].
- [16] M.-Z. Liu, Y.-W. Pan, Z.-W. Liu, T.-W. Wu, J.-X. Lu, and L.-S. Geng, Phys. Rept. **1108**, 1 (2025), arXiv:2404.06399 [hep-ph].
- [17] Z.-G. Wang, (2025), arXiv:2502.11351 [hep-ph].
- [18] T. Barnes and E. S. Swanson, Phys. Rev. C **77**, 055206 (2008), arXiv:0711.2080 [hep-ph].
- [19] P. G. Ortega, D. R. Entem, and F. Fernandez, J. Phys. G **40**, 065107 (2013), arXiv:1205.1699 [hep-ph].
- [20] S. Kanwal, F. Akram, B. Masud, and E. S. Swanson, Eur. Phys. J. A **58**, 219 (2022), arXiv:2211.08015 [hep-ph].
- [21] Q. Deng, R.-H. Ni, Q. Li, and X.-H. Zhong, Phys. Rev. D **110**, 056034 (2024), arXiv:2312.10296 [hep-ph].
- [22] Z.-L. Man, C.-R. Shu, Y.-R. Liu, and H. Chen, Eur. Phys. J. C **84**, 810 (2024), arXiv:2402.02765 [hep-ph].
- [23] Z.-H. Pan, C.-X. Liu, Z.-L. Man, and X. Liu, (2024), arXiv:2411.15689 [hep-ph].
- [24] Y. Yamaguchi, A. Hosaka, S. Takeuchi, and M. Takizawa, J. Phys. G **47**, 053001 (2020), arXiv:1908.08790 [hep-ph].
- [25] T. Ji, X.-K. Dong, M. Albaladejo, M.-L. Du, F.-K. Guo, J. Nieves, and B.-S. Zou, Sci. Bull. **68**, 688 (2023), arXiv:2212.00631 [hep-ph].
- [26] J. Song, L. R. Dai, and E. Oset, Phys. Rev. D **108**, 114017 (2023), arXiv:2307.02382 [hep-ph].
- [27] T. Kinugawa and T. Hyodo, Phys. Rev. C **109**, 045205 (2024), arXiv:2303.07038 [hep-ph].
- [28] P.-P. Shi, M. Albaladejo, M.-L. Du, F.-K. Guo, and J. Nieves, (2024), arXiv:2410.19563 [hep-ph].
- [29] C. Meng and K.-T. Chao, Phys. Rev. D **75**, 114002 (2007), arXiv:hep-ph/0703205.
- [30] Y.-J. Zhang, G. Li, and Q. Zhao, Phys. Rev. Lett. **102**, 172001 (2009), arXiv:0902.1300 [hep-ph].
- [31] F.-K. Guo, C. Hanhart, G. Li, U.-G. Meissner, and Q. Zhao, Phys. Rev. D **83**, 034013 (2011), arXiv:1008.3632 [hep-ph].
- [32] G. Li, X.-h. Liu, Q. Wang, and Q. Zhao, Phys. Rev. D **88**, 014010 (2013), arXiv:1302.1745 [hep-ph].
- [33] S. K. Choi *et al.* (Belle), Phys. Rev. Lett. **91**, 262001 (2003), arXiv:hep-ex/0309032.
- [34] J. Song, L. R. Dai, and E. Oset, Eur. Phys. J. A **58**, 133 (2022), arXiv:2201.04414 [hep-ph].
- [35] T. Kinugawa and T. Hyodo, Phys. Rev. C **106**, 015205 (2022), arXiv:2205.08470 [hep-ph].
- [36] Z.-Z. Song, C. Meng, Y.-J. Gao, and K.-T. Chao, Phys. Rev. D **69**, 054009 (2004), arXiv:hep-ph/0309105.
- [37] C. Meng, Y.-J. Gao, and K.-T. Chao, Phys. Rev. D **87**, 074035 (2013), arXiv:hep-ph/0506222.
- [38] Q. Wu, M.-Z. Liu, and L.-S. Geng, Eur. Phys. J. C **84**, 147 (2024), arXiv:2304.05269 [hep-ph].
- [39] R. Aaij *et al.* (LHCb), Phys. Rev. D **102**, 092005 (2020), arXiv:2005.13419 [hep-ex].

- [40] M. Ablikim *et al.* (BESIII), Phys. Rev. Lett. **132**, 151903 (2024), arXiv:2309.01502 [hep-ex].
- [41] J.-M. Xie, M.-Z. Liu, and L.-S. Geng, Phys. Rev. D **107**, 016003 (2023), arXiv:2207.12178 [hep-ph].
- [42] M.-Z. Liu and Q. Wu, Eur. Phys. J. C **85**, 188 (2025), arXiv:2409.06539 [hep-ph].
- [43] Z. Yu, Q. Wu, and D.-Y. Chen, Phys. Rev. D **111**, 014033 (2025), arXiv:2408.05813 [hep-ph].
- [44] F.-S. Yu, H.-Y. Jiang, R.-H. Li, C.-D. Lü, W. Wang, and Z.-X. Zhao, Chin. Phys. **C42**, 051001 (2018), arXiv:1703.09086 [hep-ph].
- [45] Y.-K. Hsiao, Y. Yu, and B.-C. Ke, Eur. Phys. J. C **80**, 895 (2020), arXiv:1909.07327 [hep-ph].
- [46] Z.-D. Duan, J.-P. Wang, R.-H. Li, C.-D. Lv, and F.-S. Yu, (2024), arXiv:2412.20458 [hep-ph].
- [47] S. Navas *et al.* (Particle Data Group), Phys. Rev. D **110**, 030001 (2024).
- [48] S. Godfrey and N. Isgur, Phys. Rev. D **32**, 189 (1985).
- [49] T. Barnes, S. Godfrey, and E. S. Swanson, Phys. Rev. D **72**, 054026 (2005), arXiv:hep-ph/0505002.
- [50] B.-Q. Li and K.-T. Chao, Phys. Rev. D **79**, 094004 (2009), arXiv:0903.5506 [hep-ph].
- [51] Z.-Y. Zhou, C.-Y. Li, and Z. Xiao, (2023), arXiv:2304.07052 [hep-ph].
- [52] N. Hüsken, R. F. Lebed, R. E. Mitchell, E. S. Swanson, Y.-Q. Wang, and C.-Z. Yuan, Phys. Rev. D **109**, 114010 (2024), arXiv:2404.03896 [hep-ph].
- [53] T.-C. Peng, Z.-Y. Bai, J.-Z. Wang, and X. Liu, Phys. Rev. D **111**, 054023 (2025), arXiv:2412.11096 [hep-ph].
- [54] H.-X. Chen, Phys. Rev. D **105**, 094003 (2022), arXiv:2103.08586 [hep-ph].
- [55] S. Mantry, D. Pirjol, and I. W. Stewart, Phys. Rev. D **68**, 114009 (2003), arXiv:hep-ph/0306254.
- [56] A. K. Leibovich, Z. Ligeti, I. W. Stewart, and M. B. Wise, Phys. Lett. B **586**, 337 (2004), arXiv:hep-ph/0312319.
- [57] P. Colangelo, F. De Fazio, and T. N. Pham, Phys. Lett. B **542**, 71 (2002), arXiv:hep-ph/0207061.
- [58] H.-Y. Cheng, C.-K. Chua, and A. Soni, Phys. Rev. D **71**, 014030 (2005), arXiv:hep-ph/0409317.
- [59] P. Colangelo, F. De Fazio, and T. N. Pham, Phys. Rev. D **69**, 054023 (2004), arXiv:hep-ph/0310084.
- [60] Z.-G. Wang, Eur. Phys. J. C **58**, 245 (2008), arXiv:0808.2114 [hep-ph].
- [61] H. Xu, X. Liu, and T. Matsuki, Phys. Rev. D **94**, 034005 (2016), arXiv:1605.04776 [hep-ph].
- [62] C.-D. Lu, Y.-M. Wang, H. Zou, A. Ali, and G. Kramer, Phys. Rev. D **80**, 034011 (2009), arXiv:0906.1479 [hep-ph].
- [63] H.-Y. Cheng, C.-K. Chua, and C.-W. Hwang, Phys. Rev. D **69**, 074025 (2004), arXiv:hep-ph/0310359.
- [64] R. C. Verma, J. Phys. G **39**, 025005 (2012), arXiv:1103.2973 [hep-ph].
- [65] P.-P. Shi, V. Baru, F.-K. Guo, C. Hanhart, and A. Nefediev, Chin. Phys. Lett. **41**, 031301 (2024), arXiv:2312.05389 [hep-ph].
- [66] A. Ali, G. Kramer, and C.-D. Lu, Phys. Rev. D **58**, 094009 (1998), arXiv:hep-ph/9804363.
- [67] Q. Qin, H.-n. Li, C.-D. Lü, and F.-S. Yu, Phys. Rev. D **89**, 054006 (2014), arXiv:1305.7021 [hep-ph].
- [68] R. L. Workman *et al.* (Particle Data Group), PTEP **2022**, 083C01 (2022).
- [69] S. Aoki *et al.* (Flavour Lattice Averaging Group), Eur. Phys. J. C **80**, 113 (2020), arXiv:1902.08191 [hep-lat].
- [70] Y. Li, P. Maris, and J. P. Vary, Phys. Rev. D **96**, 016022 (2017), arXiv:1704.06968 [hep-ph].
- [71] H.-n. Li, C.-D. Lu, and F.-S. Yu, Phys. Rev. D **86**, 036012 (2012), arXiv:1203.3120 [hep-ph].

- [72] Y.-s. Oh, T. Song, and S. H. Lee, Phys. Rev. C **63**, 034901 (2001), arXiv:nucl-th/0010064.
- [73] M. E. Bracco, M. Chiapparini, F. S. Navarra, and M. Nielsen, Prog. Part. Nucl. Phys. **67**, 1019 (2012), arXiv:1104.2864 [hep-ph].
- [74] Z.-w. Lin and C. M. Ko, Phys. Rev. C **62**, 034903 (2000), arXiv:nucl-th/9912046.
- [75] R.-Q. Qian and X. Liu, Phys. Rev. D **108**, 094046 (2023), arXiv:2308.14072 [hep-ph].
- [76] T. Mehen and D.-L. Yang, Phys. Rev. D **85**, 014002 (2012), arXiv:1111.3884 [hep-ph].
- [77] F.-K. Guo, C. Hanhart, and U.-G. Meissner, Phys. Rev. Lett. **103**, 082003 (2009), [Erratum: Phys.Rev.Lett. 104, 109901 (2010)], arXiv:0907.0521 [hep-ph].
- [78] G. Li and Q. Zhao, Phys. Rev. D **84**, 074005 (2011), arXiv:1107.2037 [hep-ph].
- [79] Y.-J. Zhang and Q. Zhao, Phys. Rev. D **81**, 034011 (2010), arXiv:0911.5651 [hep-ph].
- [80] N. N. Achasov and G. N. Shestakov, Phys. Rev. D **103**, 076017 (2021), arXiv:2102.03738 [hep-ph].
- [81] M. Bayar, N. Ikeno, and E. Oset, Eur. Phys. J. C **80**, 222 (2020), arXiv:1911.12715 [hep-ph].
- [82] J. He and D.-Y. Chen, Eur. Phys. J. C **79**, 887 (2019), arXiv:1909.05681 [hep-ph].
- [83] Q. Wu, D.-Y. Chen, and T. Matsuki, Eur. Phys. J. C **81**, 193 (2021), arXiv:2102.08637 [hep-ph].
- [84] Q. Wu and D.-Y. Chen, Phys. Rev. D **100**, 114002 (2019), arXiv:1906.02480 [hep-ph].
- [85] C.-P. Jia, H.-Y. Jiang, J.-P. Wang, and F.-S. Yu, JHEP **11**, 072 (2024), arXiv:2408.14959 [hep-ph].
- [86] J.-P. Wang and F.-S. Yu, Chin. Phys. C **48**, 101002 (2024), arXiv:2407.04110 [hep-ph].
- [87] C.-Q. Geng, X.-N. Jin, and C.-W. Liu, (2025), arXiv:2502.12770 [hep-ph].